Ethylene/Vinyl Acetate Copolymers via Acyclic Diene Metathesis Polymerization. Examining the Effect of "Long" Precise Ethylene Run Lengths

Mark D. Watson and Kenneth B. Wagener*

The George and Josephine Butler Polymer Research Laboratory, Department of Chemistry, University of Florida, P.O. Box 117200, Gainesville, Florida 32611-7200

Received December 9, 1999

ABSTRACT: Tandem acyclic diene metathesis (ADMET) polymerization/catalytic hydrogenation has been exploited to synthesize copolymers modeling ethylene/vinyl acetate (EVA) materials. A series of four sequence-ordered ethylene-*co*-vinyl acetate copolymers were prepared possessing precisely defined ethylene run lengths from 18 to 26 carbons. Use of the well-defined ADMET reaction in combination with a quantitative olefin−hydrogen technique generates well-defined EVA's, all of which are semicrystalline with a linear relationship between ethylene run length and melting temperature. All polymers except that with the lowest ethylene run length are film and fiber forming.

Introduction

Ethylene/vinyl acetate (EVA) copolymers constitute the world's largest volume ethylene copolymer, due in no small part to the technical significance of the post-polymerization hydrolysis to ethylene vinyl alcohol copolymers.[1] EVA's are produced commercially by the same high-pressure free radical processes utilized for low-density polyethylene. This is a special case of an ideal copolymerization, termed Bernoullian, where the reactivity ratio product $r_1r_2 \cong 1.0$ and $r_1 \cong r_2 \cong 1.0$. Monomer incorporation is truly random, and more significantly, the copolymer constitution is the same as the feed ratio, allowing the preparation of EVA's with a broad range of compositions. The ready availability of EVA's with tailored VA content has made this copolymer system ideal for studying copolymer composition/property and morphology relationships, and as a result, much physical data have accumulated for these copolymers.[1,2] Therefore, EVA's not only represent a highly versatile class of practical materials, they have also served as a valuable tool for gaining fundamental knowledge of polymer behavior.

However, as a result of the nature of the free radical polymerization, the polymer microstructures are ill-defined with uncontrolled branching and broad polydispersities due to chain transfer reactions. In addition to the typical branch-producing reactions in the free radical polymerization of ethylene, both the methine proton of the vinyl acetate repeat unit and the methyl protons of the acetoxy group in either the monomer or the repeat unit provide sites for additional branching with moderately high chain transfer constants.[3] A recent study of the morphology of representative commercial EVA's discloses that in some cases the total number of branches can be up to twice the acetate content of the polymer.[2a] In studies aimed at delineating the effect of the incorporated acetate comonomers, evaluation of physical measurements must surely be clouded by the ill-defined microstructures. From a technical point of view, increased understanding of these relationships is important for the rational manufacture of materials with tailored physical properties that depend on copolymer microstructural details such as sequence distribution, identity of comonomer, and contributions from branching inherent in the chain polymerizations. On a more fundamental level, valuable knowledge of polymer crystallization as well as glass and subglass transitions[2c,d] related to mobility of polymer-bound substituents could be gained with the availability of model polymers with more well-defined microstructures.

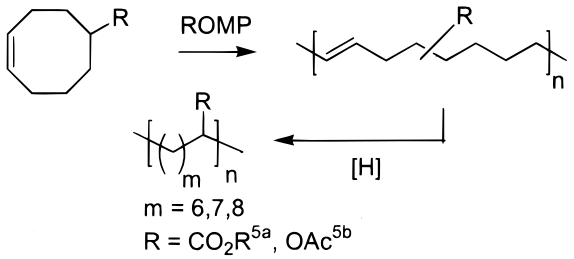

Figure 1. Synthesis of ethylene polar monomer copolymers via ROMP and hydrogenation.

A number of model sequence-ordered ethylene/polar monomer copolymers (EPM) have been synthesized in order that they may be compared with their random counterparts. Polymers with regular ethylene sequences greater than one have only been prepared by post-polymerization modification. Examples include polymers with ethylene−ethylene−polar monomer sequences, which are produced via hydrogenation of alternating copolymers of butadiene and polar monomers.[4] This method is however limited to the preparation of polymers with substituents separated by a maximum of five carbons.

Further advances to longer ethylene run lengths have been achieved through ring-opening metathesis polymerization (ROMP) of substituted cycloolefins, again followed by hydrogenation (Figure 1).[5] Both examples in Figure 1 are particularly relevant, as the first[5a] revealed a synthetic route similar to that reported here in which a ruthenium complex is used for both metathesis and hydrogenation and the second[5b] produces a model EVA polymer. The clean nature of the metathesis reaction with well-defined metal complexes guarantees that the polymers are entirely branch-free except for the

10.1021/ma9920689 CCC: $19.00
Published on Web 06/24/2000

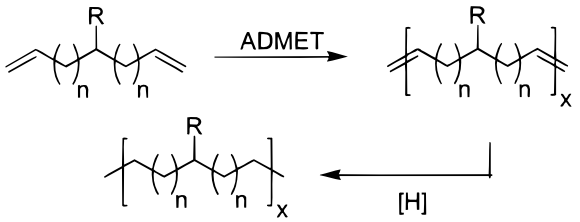

Figure 2. Synthesis of sequence ordered ethylene copolymers via ADMET and hydrogenation.

branches incorporated into the monomer. The polymers shown, however, cannot be regioregular due to the asymmetry of the monomers. For example, the pendant substituents in the polymers prepared from cyclooctene derivatives may be separated by 6, 7, and 8 carbons depending on the mode of insertion of the monomer. Similar methodologies[6] have incorporated substituted cyclododecadiene-derived polymers, but the sequence distributions are perhaps even further complicated by the availability of two reactive sites during the ROMP reaction. However, due to the branch-free nature of the polymers and the moderately high control over sequence distribution, these polymers represent a bridge between the commercial EPM copolymers and the perfectly sequence controlled polymers which we report here.

Recently, we reported a method for preparing perfectly sequence ordered ethylene−propylene copolymers by acyclic diene metathesis (ADMET) chemistry followed by stoichiometric diimide reduction (Figure 2, R = CH_3).[7] The ADMET reaction is similar to ROMP in that entirely linear polymers are produced where the only branching present is dictated by the pendant substituents incorporated into the monomer. If symmetric diene monomers are used, the only irregularity is the cis/trans stereochemistry of the backbone olefinic linkages. Hydrogenation of these sites removes this sole irregularity and produces polymers with precisely controlled repeating sequences. Further, the ethylene run lengths may be easily dictated during the monomer synthesis by changing the value of "n" in Figure 2.

More recently, we have developed a tandem process[8] where the ruthenium metathesis catalyst, $Cl_2(Cy_3P)_2$-RuCHPh (**1**),[9] is utilized for ADMET polymerization and then is converted in situ to an effective heterogeneous olefin hydrogenation catalyst. This method streamlines our ADMET/hydrogenation approach to the syntheses of sequence-ordered ethylene copolymers. The aforementioned abundance of available data concerning structure−property relations of commercial EVA's prompted us to begin our modeling studies of *functionalized* ethylene polymers with this class of materials. In this paper, we report the use of this process to prepare a series of model ethylene-*co*-vinyl acetate (Figure 2, R = OAc) polymers with precisely defined ethylene run lengths from 18 up to 26 carbons.

Results and Discussion

Monomer Synthesis. The synthesis of polymers with "long" ethylene run lengths by this method requires dienes with a correspondingly large number of methylene spacers between the vinyl groups and the central functionality. Symmetric dienes with central pendant acetoxy groups were synthesized in good yields via acetylation of secondary alcohols (Figure 4). The shortest alcohol functional diene (**8**, $n = 8$) was prepared by LAH reduction of ketone diene (**7**).[8] The remaining

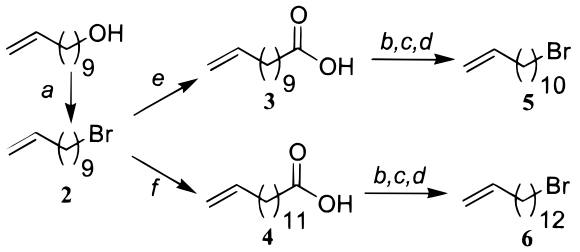

Figure 3. Syntheses of ω-alkenyl bromides: *a*, Ph_3P, CBr_4; *b*, LAH; *c*, TsCl, pyr; *d*, LiBr, acetone; *e*, Mg, CO_2; *f*, Mg, CuCl, β-propiolactone.

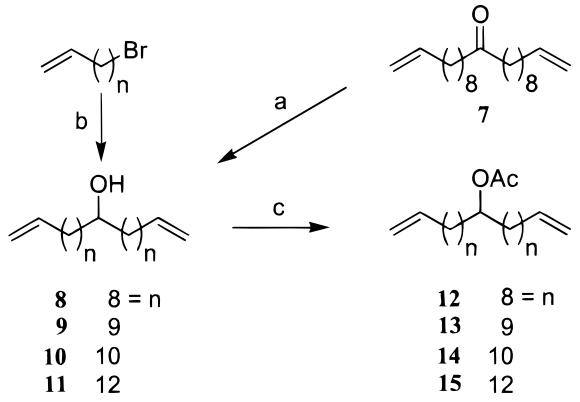

Figure 4. Syntheses of acetoxy-functional diene monomers: *a*, LAH; *b*, Mg, 0.5 equiv of HCO_2Me; *c*, AcCl or Ac_2O, pyr.

secondary alcohols ($n = 9$, 10, and 12) were prepared in good yields in one step via reaction of ω-alkenyl Grignard reagents with methyl formate. These ω-alkenyl bromides were prepared as outlined in Figure 3. The chain extension reactions, transforms $e + b$ or $f + b$ in Figure 3, could also each be achieved in one step by substituting formaldehyde and oxirane respectively for CO_2 and β-propiolactone. However, the ω-unsaturated acid intermediates are useful starting materials for preparing additional dienes from which other model polymers were prepared, to be published later. All four acetoxy-functional monomers prepared for this study were obtained in sufficient purity that contaminants could not be detected by GC, HPLC (normal phase, UV, and IR detectors), and NMR.

Polymer Synthesis and Characterization. Each of the model polymers was prepared by our tandem homogeneous ADMET/heterogeneous hydrogenation approach.[8] Monomer and catalyst **1** (400:1) were combined inside an argon-purged drybox, and the ADMET polymerization was then conducted at 45−65 °C (48 h) under reduced pressure utilizing standard Schlenk techniques. The resulting reaction mixture of ADMET polymer/catalyst residue was combined with silica (100 times the weight of ruthenium catalyst), and olefin hydrogenation was conducted in toluene at 90 °C under 120 psig H_2. Although ^1H NMR experiments indicate that the reaction is complete in 5−6 h, hydrogenations were conducted over a period of 24 h to ensure maximum reduction. The catalyst residue/silica composite was filtered from solution, and the toluene was evaporated under reduced pressure to yield the white polymers in virtually quantitative yield. With the exception of the polymer **HP12**, the polymers yield tough films and fibers from solution or from the melt, and optically transparent or translucent articles may be obtained from the melt. The low T_m (approximately RT) of **HP12** precludes any "form stability" at room temperature.

Table 1. Characterization of ADMET EVA Model Polymers

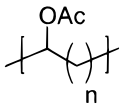

polymer	"*n*"	$M_n \times 10^{-4}$ (g/mol)[a]	T_m (°C)
HP12	18	4.0	23
HP13	20	3.1	35
HP14	22	4.9	41
HP15	26	6.6	57[b]

[a] GPC versus polystyrene. For all cases, PDI = 1.8. [b] Crystallized from melt, 49 °C(5 h). T_m (unannealed) = 55 °C.

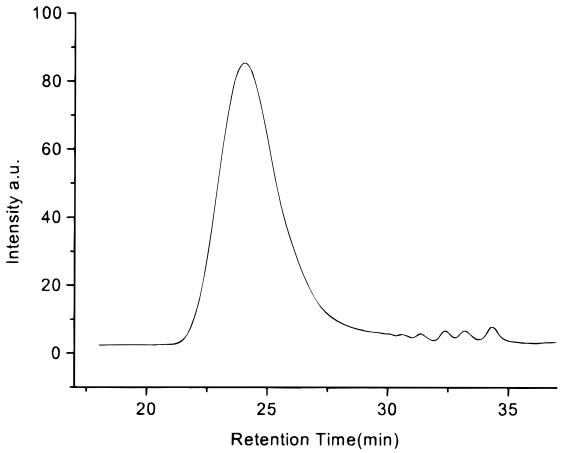

Figure 5. GPC trace of **HP15** showing oligomers.

If these polymers are to serve as true models for EVA copolymers, they must exhibit high molecular weights in addition to pure repeating microstructures. The realization of practical molecular weights is confirmed by GPC analysis, where all four polymers show values in the range (3−7) × 10^4 g/mol (Table 1). The typical GPC trace shown in Figure 5 clearly illustrates the condensation nature of these model EVA polymers. As is usually the case, the ADMET polymerization produces a monomodal, moderate molecular weight product mixture with the most probable distribution (PDI ≅ 2) as well as cyclic oligomers inevitably produced during the condensation of nonrigid bifunctional monomers. The series of small peaks, with M_p differing by a few hundred mass units, most likely represent cyclic oligomers which are apparently resolved by the GPC column due to the long linear dimension of the repeat unit.

As mentioned previously, in regards to the most important requirement of high homogeneity for model polymers, the only variable in the repeat structure of ADMET polymers prepared from symmetric monomers is the cis/trans stereochemistry of the backbone olefinic linkages, and this is eliminated upon hydrogenation. As can be seen in Figure 6, hydrogenation greatly simplifies the ^{13}C spectrum as a result of the degeneration of chemical environments distal to the acetate group. Examination of the olefin region in the spectra illustrates that the method for hydrogenation is exhaustive within spectroscopic detection limits as indicated by complete disappearance of signals at ∼130 ppm; the corresponding signals in the ^1H spectra (∼5.3−5.5 ppm) are also eliminated. All spectra for the remaining EVA models are identical, regardless of ethylene run length, aside from changes in the ^1H integrals corresponding to decreasing acetate content.

The pattern of peaks in the ^{13}C spectra of the model EVA's is characteristic of all the model polymers we have prepared by this method regardless of the pendant functionality. In addition to peaks attributed to the pendant group and the methine carbon, the only other peaks are a partially resolved cluster at ∼30 ppm ("f" in Figure 6, lower spectra) and signals slightly downfield and upfield relative to "f" for the carbons α and β, respectively, to the methine carbon. The cluster of peaks "f" may be partially resolved to 3−4 peaks (at 75 MHz) and corresponds to backbone carbons (polyethylene segments) more than twice removed from the methine carbon.

Thermal Characterization. The physical properties of EVA copolymers can be tailored by varying the VA content to fit applications as diverse as hot melt adhesives, packaging films, and rubbery toys.[1] Melting point depression upon inclusion of a noncrystallizable repeat unit into a crystallizable backbone is a general phenomenon, and EVA copolymers are no exception, where the degree of depression is proportional to the comonomer content. This phenomenon was treated theoretically by Flory (exclusion model)[10] and described by the well-known eq 1. The equation describes the observed melting point (T_m) as a function of the mole fraction of noncrystallizable groups (X_b) where T_m^0 is the theoretical maximum melting point of the crystalline homopolymer and ΔH_m^0 is the heat of fusion per crystallizable repeat unit. While this equation adequately describes the generally observed *trends* in melting point depression, it underestimates the *magnitude* of depression. This treatment is complemented by the inclusion model proposed by Eby and Sanchez.[11]

$$T_m = T_m^0\left(1 - \frac{R T_m^0}{\Delta H_m^0} X_b\right) \qquad (1)$$

Not surprisingly, the trend of decreasing T_m (DSC) with increasing VA content was observed with these model EVA polymers. As expected on the basis of our results concerning model sequence-ordered ADMET ethylene/propylene copolymers,[7] each of the polymers displayed sharper melting transitions relative to commercial analogues due to greater chemical homogeneity. The melting transitions of commercial analogues may span up to 50 °C, typical of semicrystalline random copolymers with a broad range of crystalline morphologies ascribed to chemical inhomogeneity.

The samples in this study were heated to 100 °C to erase thermal history and then scanned at 5 °C/min, cooling cycle first, to locate thermal transitions. On cooling, all polymers displayed a first-order, sharp exotherm, spanning <15 °C (inset, Figure 7). On the heating cycle, a broader endotherm with a shoulder on the high-temperature side was observed (Figure 7). The difference between the peak temperatures for the two major transitions on cooling and heating, assigned as T_c and T_m, respectively, was ≤20 °C. The onset of the T_m is unclear due to observed premelting indicated by the slope of the baseline leading up to the peak. The endotherms are broader and less defined and occur at lower temperatures than the analogous ADMET methyl-substituted polyethylenes.[7] Undoubtedly, this is a consequence of the greater steric bulk of the acetoxy groups relative to methyl.

Annealing at temperatures just below the melting point affects the positions and shapes of the melting

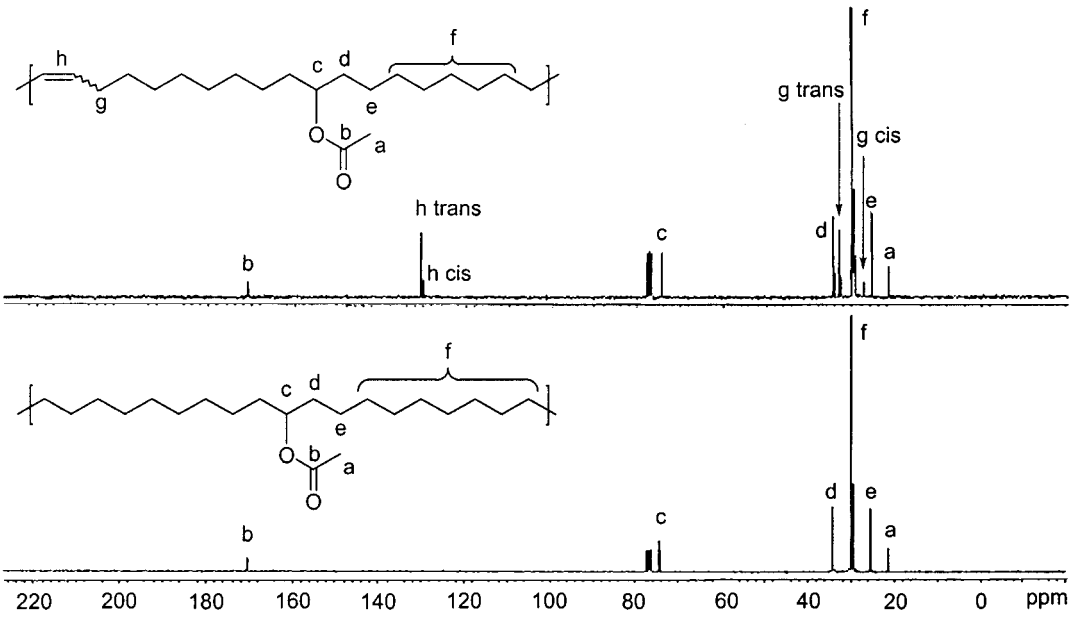

Figure 6. ^{13}C NMR spectra of **HP12** (bottom) and its unsaturated precursor (top).

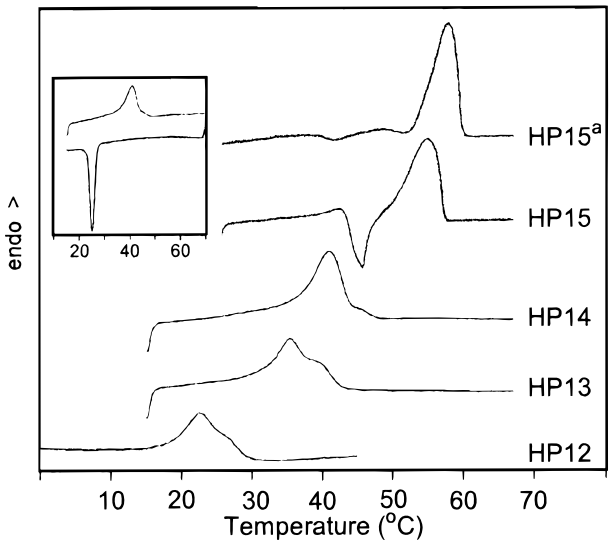

Figure 7. DSC heating curves of ADMET EVA polymers (5 °C/min after cooling from 100 °C at 5 °C/min). Inset is heating and cooling trace for HP14. a: crystallized from melt (49 °C, 5 h).

endotherms in typical fashion. Peak T_m increases with increasing annealing temperature, and the peak sharpens as the baseline preceding the endotherm flattens, a consequence of producing a more highly crystalline sample. The peak T_m may ultimately be shifted to a position that overlaps the high-temperature shoulders seen in the scans of unannealed samples.

The DSC trace of **HP15** reveals thermal behavior not observed with the other polymers with shorter ethylene run lengths. The exothermic peak on the heating cycle just prior to the T_m indicates cold crystallization. This phenomenon, first theoretically treated by Wunderlich,[12] is most effectively observed after a crystalline polymer is quenched from above T_m to below T_g, minimizing crystallization on cooling. Upon heating to a given temperature between T_g and T_m, crystallization ensues. The rate of crystallization for **HP15** may be significantly slower than for the other EVA's, diminishing the effective crystallization which occurs during the cooling scan. On the subsequent heating cycle, more of the amorphous material then crystallizes rapidly just below T_m. Annealing just below T_m all but eliminates the sharp exotherm in the subsequent heating scan (top curve, Figure 7).

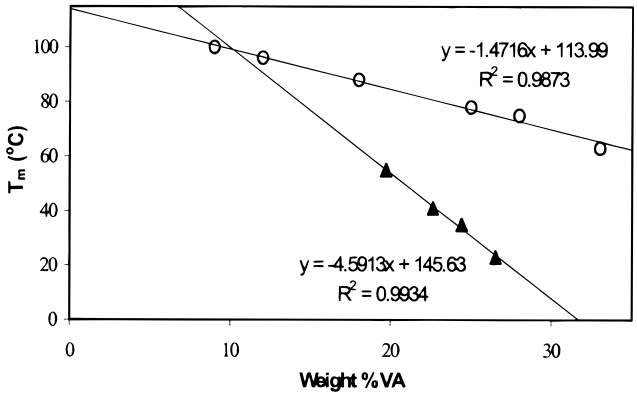

Figure 8. Plot of T_m vs wt % VA: (▲) ADMET EVA copolymers (5 °C/min); (○) Elvax series commercial EVA (10 °C/min).[13]

The melting points (unannealed) of the ADMET EVA polymers are plotted versus weight percent VA together with the values reported[13] for the commercially available Elvax series (Figure 8). These are plotted by weight percent for comparison and for simplification rather than attempting to define the "noncrystallizable unit" necessary for use of eq 1. It should be noted that the values for the commercial resins were obtained at a slightly faster heating rate (10 vs 5 °C/min), but this does not account for the drastic differences illustrated in the figure. Like the commercial resins, the relationship is linear ($R^2 = 0.99$) in the region studied. The values are consistently lower for the model polymers, and the absolute value for the slope of the line is approximately 3 times that of the commercial resins. The *y*-intercept, corresponding to 0% VA, for the commercial resins is 114 °C, which is very close to the reported T_m = 110 °C for the parent low-density polyethylene prepared under the same conditions. Although it may be purely coincidental, the intercept for the model EVA's (145.6 °C) very closely approaches the theoretical value[14] for perfectly linear polyethylene.

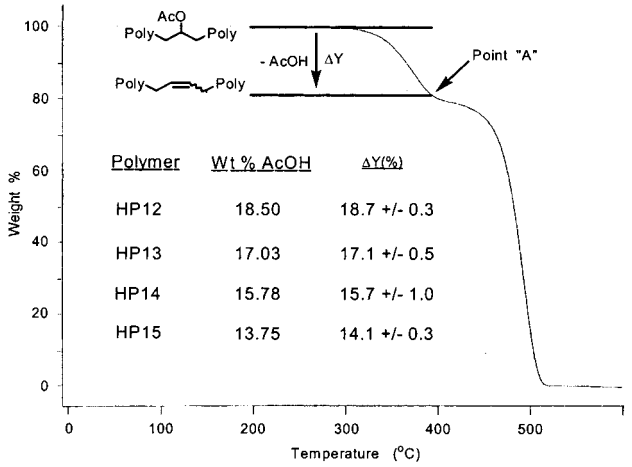

Figure 9. TGA trace for **HP12** showing typical two-stage weight loss. Tabulated values reported for ΔY (elimination of AcOH) are averages of three runs.

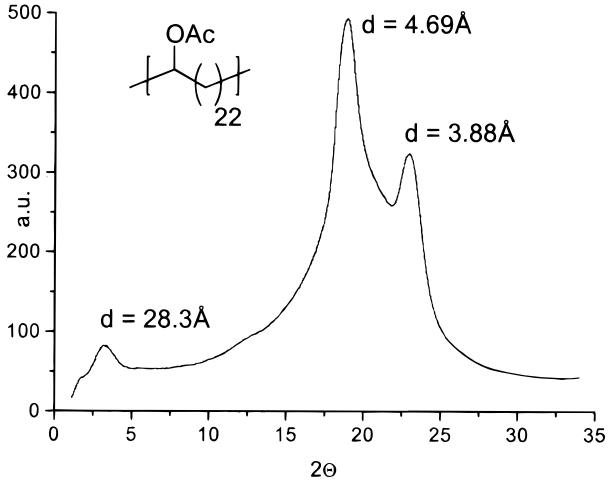

Figure 10. Preliminary WAXS characterization of **HP14**. Cooled at 5 °C/min from 70 °C to room temperature.

Further studies with longer ethylene run lengths would reveal whether this relation holds over a greater copolymer composition range and under the more rigorous DSC studies designed to obtain true equilibrium melting points.

Upon heating to approximately 300 °C, acetic acid is thermally eliminated from the polymer backbone of EVA's, and this is the source of the upper limit for processing and end use temperatures. Measurement of weight loss due to this reaction by TGA is a useful technique for measuring the acetate content of EVA copolymers.[15] A representative TGA plot (**HP12**) is shown in Figure 9, illustrating the stepwise weight loss due to this elimination reaction followed by catastrophic decomposition. The transition between the weight loss due to thermal elimination of AcOH and the onset of further decomposition was not a distinct step, nor did it occur at the exactly same temperature for each run. Instead, the end of the first step was taken as the inflection point, labeled as "A" in Figure 9, digitally calculated for each run. Excellent agreement is seen in the tabulated predicted and measured percent weight loss (average of triplicate measurements) due to thermal elimination of acetic acid for each polymer, also included in the figure.

Given the extremely high microstructural purity of these polymers, the intriguing question arises of whether, and to what extent, the bulky pendant acetate groups might be arranged within a crystalline array. Preliminary WAXS experiments suggest that the acetate groups are indeed ordered to some degree in bulk samples. The small diffraction peak in the low-angle region of Figure 10 (**HP14**) indicates a regularly spaced element with *d* spacing of approximately 28 Å, which corresponds very closely with the length of the polyethylene segments of this polymer. More detailed studies will follow with the aim of delineating the crystallographic nature of these polymers.

Conclusions

Perfectly sequence-ordered, branch-free model EVA polymers may be prepared by the combination of ADMET polymerization and hydrogenation. All microstructural variables present in commercial polymers are eliminated, and the ethylene run length is easily defined during the monomer synthesis. As expected on the basis of previous practical and theoretical treatments of random copolymers, there is a linear relation between comonomer content and melting point. These polymers should allow the more accurate evaluation of copolymer structure−property relationships related to the identity and concentration of comonomers as applied studies follow. In a continuing effort to provide a range of sequence-ordered polymers for such studies, we have also prepared analogous ethylene/polar monomer copolymers containing acrylates, acrylic acids, vinyl chloride, and styrene.

Experimental Section

A. General Considerations. ^{1}H NMR (300 MHz) and ^{13}C NMR (75 MHz) spectra were recorded on a Gemini series NMR superconducting spectrometer system or a Varian VXR-300 in $CDCl_3$. Resonances are referenced to residual protio solvent and reported in δ units downfield from TMS at 0.0 ppm. Elemental analysis was performed by Atlantic Microlab, Inc., Norcross, GA. Low-resolution mass spectrometry data were recorded on a Finnigan MAT 95Q gas chromatograph/mass spectrometer utilizing electron ionization. Gel permeation chromatography (GPC) was performed using a Waters Associates liquid chromatograph U6K equipped with tandem ABI Spectraflow 757 UV absorbance detector and a Perkin-Elmer LC-25 RI detector. The GPC solvent delivery system was configured for elution with THF through an Ultrastyragel linear mixed bed column at a rate of 1.0 mL/min. Retention times were calibrated against eight narrow (PDI < 1.07) polystyrene standards (Scientific Polymer Products, Inc) with $M_p = 1.350 \times 10^3 - 8.6 \times 10^5$ g/mol.

Differential scanning calorimetric (DSC) and thermogravimetric analysis (TGA) data were obtained with a Perkin-Elmer 7 series thermal analysis system. DSC samples (5−10 mg) were analyzed with ice as coolant and under a helium flow rate of 25 mL/min. All samples were predried at 40−50 °C under reduced pressure (<0.1 mmHg) for at least 24 h. The instrument was calibrated for peak onset temperature transitions and peak area using indium as standard. Samples were scanned at a heating/cooling rate of 5 °C/min from 10 to 100 °C with data collection during the second cycle. TGA samples (5−10 mg) were heated from room temperature at 20 °C/min under N_2 with a flow rate of 30 mL/min, until complete combustion.

B. Materials. The ruthenium catalyst (**1**) was prepared according to the literature.[9] Pyridine, toluene, and THF were distilled from Na/K alloy under argon and degassed. All other reagents were used as received. Silica gel-60 (Fischer, Selecto Scientific catalog no. 162824, particle size 32−63 μm) was sonicated twice in reagent grade $CHCl_3$, dried under reduced pressure (<0.5 mmHg) at 80 °C with magnetic agitation for 48 h, and stored in an argon-purged drybox until use.

C. Synthesis of Diene Monomers for Model EVA-Copolymers. a. Synthesis of Extended Chain ω-Alkenyl Bromides. 10-Undecenyl Bromide (2). The alkenyl bromide was prepared in two steps from the respective alcohol via the tosylate. 10-Undecenol (82.5 g, 0.484 mol, 1 equiv) was dissolved in 500 mL of $CHCl_3$ in a 1 L Schlenk flask. The solution was placed under argon and chilled to 0 °C. Pyridine (78 mL, 2 equiv) was decanted into the flask from CaH_2. Solid TsCl (138.4 g, 0.726 mol, 1.5 equiv) was added under argon in increments over ~1.5 h. After 8 h the reaction mixture was washed with water, saturated $NaHCO_3$, 3 N HCl, and brine. The organic layer was dried with Na_2SO_4 and concentrated to 154.7 g pale yellow oil which was converted to the bromide without further purification. The crude tosylate was dissolved in 900 mL of dry acetone under argon. $LiBr_{anh}$ (126 g, 3 equiv) was added in one portion, the flask was fitted with a water-cooled condenser, and the mixture was refluxed for 12 h. The mixture was filtered, diluted with 300 mL of pentane, filtered a second time, and concentrated. The crude product was taken up in 300 mL of pentane and washed with water, saturated $NaHCO_3$, and brine. The organic layer was dried with Na_2SO_4 and concentrated, and the bromide (97% GC) was vacuum transferred from CaH_2. Yield: 100.8 g, 89% for two steps. ^{1}H NMR δ (ppm): 5.80 (m, 1H); 4.95 (m, 2H); 3.40 (t, 2H); 2.04 (q, 2H); 1.85 (m, 2H); 1.38 (m) + 1.29 (br) = 12H. ^{13}C NMR δ: 139.1, 114.1, 33.96, 33.76, 32.81, 29.33, 29.04, 28.88, 28.71, 28.13.

11-Dodecenoic Acid (3). 10-Undecenyl bromide (**2**) (10 g, 42.9 mmol, 1.0 equiv) was added slowly via syringe to freshly scoured Mg turnings (1.053 g, 43.3 mmol, 1.01 equiv) in 50 mL of dry THF with rapid stirring under argon. After stirring 2 h at 45 °C, the resulting Grignard solution was rapidly poured into a large beaker containing 19 g (~10 equiv) of finely crushed CO_2(s). The mixture was stirred with 50 mL of 3 N HCl and 80 mL of pentane, after which the aqueous layer was discarded. The organic layer was washed with 3 N HCl and water, dried over Na_2SO_4, and concentrated to 8.16 g of pale yellow oil. The oil was further purified by distillation under reduced pressure (bp = 110−115 °C/0 < P < 0.1 mmHg) to yield 6.71 g of colorless oil (79% yield). ^{1}H NMR δ (ppm): 11.76 (br, 1H); 5.80 (m, 1H); 4.93 (m, 2H); 2.32 (t, 2H); 2.01 (q, 2H); 1.60 (m, 2H); 1.26 (br, 12H). ^{13}C NMR δ: 180.6, 139.1, 114.1, 34.11, 33.78, 29.67, 29.38, 29.35, 29.20, 29.07, 29.01, 28.89, 24.63.

13-Tetradecenoic Acid (4). 10-Undecenyl bromide (**2**) (22.25 g, 95.4 mmol, 1.0 equiv) was added slowly via syringe to freshly scoured Mg turnings (2.34 g, 96.2 mmol, 1.01 equiv) in 100 mL of dry THF with rapid stirring under argon. After stirring 2 h at 45 °C, the resulting Grignard solution was cooled to RT and transferred via cannula to $CuCl_{(anh)}$ (0.161 g, 1.6 mmol) in 100 mL of dry THF at 0 °C. β-Propiolactone (Acros) (5 mL, 79.5 mmol, 0.83 equiv) was added dropwise via syringe, maintaining the temperature below 5 °C. After 1 h, reaction was quenched with 50 mL of 3 N HCl and then concentrated. The crude product was taken up in 200 mL pentane and washed with 3 N HCl, water, and brine. The organic layer was dried over Na_2SO_4 and concentrated to 20.03 g (over theory) of pale yellow oil, which solidified on standing. The product was further purified by distillation under reduced pressure (bp ≅ 126 °C/0 < P < 0.1 mmHg) or by flash chromatography (20% EtOAc/pentane), rendering 85% and 91% isolated yields, respectively, of a white waxy solid. ^{1}H NMR δ (ppm): 11.22 (br, 1H); 5.79 (m, 1H); 4.92 (m, 2H); 2.32 (t, 2H); 2.02 (q, 2H); 1.61 (m, 2H); 1.24 (br, 16H). ^{13}C NMR δ: 180.6, 139.2, 114.1, 34.12, 33.80, 29.55, 29.47, 29.41, 29.22, 29.13, 29.03, 28.93, 24.64.

11-Dodecenyl Bromide (5). Following the LAH reduction of 11-dodecenoic acid (**3**) to the respective alcohol, **5** was obtained in two steps via the tosylate as described previously for preparation of **2**. Solid LAH pellets (7.34 g, 1.5 equiv) were added in increments over 1 h to **3** (25.6 g, 0.129 mol) in 300 mL of anhydrous ether under argon and stirred for 8 h. The solution was chilled below 0 °C, quenched with 300 mL of 3 N HCl, and then combined with 100 mL of ether. The organic layer was washed with 3 N HCl, water, 1 N NaOH, and brine, then dried over Na_2SO_4, and concentrated to 22.8 g of clear colorless liquid (>99% GC). The resulting 11-dodecenol was converted to the tosylate as described previously. The crude tosylate was recrystallized from MeOH/H_2O, taken up in $CHCl_3$ and dried with Na_2SO_4, and finally concentrated to 38.19 g of white solid. The toslylate was converted to **5** by the action of LiBr in refluxing acetone as described previously and purified by fractional distillation. Yield: 22.5 g, 71% overall for three steps. ^{1}H NMR δ (ppm): 5.78 (m, 1H); 4.93 (m, 2H); 3.36 (t, 2H); 2.01 (q, 2H); 1.83 (m, 2H); 1.35 (m) + 1.28 (br) = 14H. ^{13}C NMR δ: 139.1, 114.2, 33.96, 33.73, 32.79, 29.30, 29.02, 28.80, 28.67, 28.10.

13-Tetradecenyl Bromide (6) was prepared from 13-tetradecenoic acid (**4**) in three steps as previously described for the preparation of **5**, excluding recrystallization of the intermediate tosylate. The bromide was purified by flash chromatography (pentane). Yield: 56% overall for three steps.^{1}H NMR δ (ppm): 5.78 (m, 1H); 4.94 (m, 2H); 3.38 (t, 2H); 2.02 (q, 2H); 1.83 (m, 2H); 1.36 (m) + 1.25 (br) = 18H. ^{13}C NMR δ: 139.2, 114.1, 33.93, 33.81, 32.82, 29.53, 29.42, 29.13, 28.92, 28.77, 28.16.

b. Synthesis of Symmetrical Alcohol-Functionalized Dienes. 11-Hydroxy-1,20-heneicosadiene (8) was prepared by LAH reduction of crude ketone diene, 11-oxo-1,20-heneicosadiene (**7**). The ketone diene **7** was prepared as published[8] in two steps via Claisen condensation of ethyl 10-undecenoate to form the β-keto ester diene, followed by dealkoxycarbonylation without isolation of the first step. The crude ketone was dissolved in 300 mL of dry THF under argon in a 500 mL Schlenk flask equipped with an addition funnel. LAH (1 M in THF, 0.5 equiv) was added dropwise via the addtion funnel at room temperature with stirring. After 12 h, the solution was cooled to 0 °C and quenched by slow addition of 100 mL of 3 M HCl. The mixture was extracted with ether, and the ether solution was washed with saturated $NaHCO_3$ and deionized water, dried over $MgSO_4$, and concentrated to an oily off-white solid. The pure diene **8** was obtained as a white solid after flash chromatography (10% EtOAc/hexanes). Yield: 70.7% overall for three steps. ^{1}H NMR δ (ppm): 5.78 (m, 2H); 4.94 (m, 4H); 3.55 (b, 1H); 2.01 (q, 4H); 1.37 (m) + 1.25 (br) = 28H. ^{13}C NMR δ: 139.2, 114.1, 71.94, 37.45, 33.77, 29.66, 29.54, 29.42, 29.10, 28.89, 25.63.

1,22-Tricosadiene-12-ol (9). 10-Undecenyl bromide (**2**) (5 g, 21.4 mmol, 1.0 equiv) was added slowly via syringe to freshly scoured Mg turnings (0.525 g, 21.6 mmol, 1.01 equiv) in 50 mL of dry THF with rapid stirring under argon. After stirring 1 h at 45 °C, the resulting Grignard solution was chilled to 0 °C, and methyl formate (0.63 mL, 0.48 equiv) was added dropwise, while maintaining the temperature below 5 °C. The contents were warmed to RT, stirred 30 min, and then concentrated. The product mixture was taken up in pentane and 3 N HCl. The organic layer was washed with 3 N HCl and DI H_2O, dried over Na_2SO_4, and concentrated to 3.0 g of white solid. The alcohol was purified by flash chromatography (10%EtOAc/hexanes). Yield: 2.76 g, 76.6%. ^{1}H NMR δ (ppm): 5.78 (m, 2H); 4.92 (m, 4H); 3.55 (b, 1H); 2.01 (q, 4H); 1.37 (m) + 1.25 (br) = 32H. ^{13}C NMR δ: 139.2, 114.1, 71.94, 37.47, 33.77, 29.69, 29.59, 29.53, 29.46, 29.11, 28.91, 25.63.

1,24-Pentacosadiene-13-ol (10). Diene **10** was prepared by reaction of 11-dodecenylmagnesium bromide (from **5**) with methyl formate utilizing similar protocol described for preparation of diene **9**. Yield: 81.4%. NMR spectra are identical within experimental error with that of **9**.

1,28-Nonacosadiene-15-ol (11). Diene **11** was prepared by reaction of 13-tetradecenylmagnesium bromide (from **6**) with methyl formate utilizing similar protocol described for preparation of diene **9**. Yield: 79%. NMR spectra are identical within experimental error with that of **9**.

c. Synthesis of Symmetrical Dienes with Pendant Acetatoxy Groups. General Procedure for Acetylating Alcohol-Functional Dienes. The alcohol diene was weighed into a Schlenk flask and dried either by stirring in the molten state at 45−70 °C under reduced pressure (<5 mmHg) for several hours or by dissolution in dry toluene followed by evaporation under reduced pressure. Excess AcCl (4−10 equiv)

was added dropwise to a solution of the alcohol in either dry toluene or anhydrous ether containing pyridine (slight excess over that of AcCl). Both AcCl and pyridine were transferred via syringe after storage over CaH_2 under argon. After aqueous workup, the crude acetates were purified by flash chromatography (2−3% EtOAc/pentane or hexanes). Products obtained in this manner were free of detectable impurities (HPLC, GC, NMR) with the exception of 15-acetoxy-1,28-nonacosadiene (**15**) which required further purification by HPLC (normal phase, 2% EtOAc/hexanes) to separate impurities with nearly identical R_f values.

11-Acetoxy-1,20-heneicosadiene (12) was prepared as described above from **8**. Yield: 82%, clear, colorless oil (100% GC). LRMS: 351 (m+). Elem. Anal. Calcd for $C_{23}H_{42}O_2$: C, 78.80; H, 12.08. Found: C, 78.82; H, 12.21. ^{1}H NMR δ (ppm): 5.77 (m, 2H); 4.94 (m) + 4.83 (p) = 5H; 2.02 (q) + 1.99 (s) = 7H; 1.46 (m, 4H); 1.34 (m) + 1.23 (br) = 24H. ^{13}C NMR δ: 170.7, 139.0, 114.0, 74.27, 34.05, 33.73, 29.41, 29.33, 29.03, 28.85, 25.24, 21.15.

12-Acetoxy-1,22-tricosadiene (13) was prepared as described above from **9**. Yield: 86%, clear, colorless oil (100% GC). LRMS: 378 (m+). Elem. Anal. Calcd for $C_{25}H_{46}O_2$: C, 79.30; H, 12.25. Found: C, 79.25; H, 12.29. ^{1}H NMR δ (ppm): 5.77 (m, 2H); 4.94 (m) + 4.83 (p) = 5H; 2.02 (q) + 1.99 (s) = 7H; 1.46 (m, 4H); 1.34 (m) + 1.23 (br) = 28H. ^{13}C NMR δ: 170.8, 139.1, 114.1, 74.36, 34.10, 33.76, 29.47, 29.42, 29.09, 28.91, 25.28, 21.23.

13-Acetoxy-1,24-pentacosadiene (14) was prepared as described above from **10**. Yield: 93%, clear, colorless oil (100% GC). LRMS: 406 (m+). Elem. Anal. Calcd for $C_{27}H_{50}O_2$: C, 79.74; H, 12.39. Found: C, 79.81; H, 12.45. ^{1}H NMR δ (ppm): 5.77 (m, 2H); 4.94 (m) + 4.83 (p) = 5H; 2.02 (q) + 1.99 (s) = 7H; 1.46 (m, 4H); 1.34 (m) + 1.23(br) = 32H. ^{13}C NMR δ: 170.9, 139.1, 114.1, 74.36, 34.15, 33.70, 29.49, 29.43, 29.03, 28.85, 25.24, 21.17.

15-Acetoxy-1,28-nonacosadiene (15) was prepared as described above from **11**. Yield: 62%, white solid (100% GC). LRMS: 463 (m+1). Elem. Anal. Calcd for $C_{31}H_{58}O_2$: C, 80.45; H, 12.63. Found: C, 80.39; H, 12.75. ^{1}H NMR δ (ppm): 5.78 (m, 2H); 4.93 (m) + 4.80 (p) = 5H; 2.02 (q) + 2.00 (s) = 7H; 1.47 (m, 4H); 1.33 (m) + 1.23 (br) = 40H. ^{13}C NMR δ: 170.9, 139.2, 114.1, 74.41, 34.10, 33.81, 29.62, 29.60, 29.56, 29.53, 29.50, 29.14, 28.93, 25.30, 21.28.

D. Synthesis of ADMET Model EVA Copolymers. General Procedure for Polymerization and Hydrogenation. The pure diene monomers may be adequately dried and degassed by replacing the atmosphere three times with argon via three successive pump/purge cycles and then stirring under reduced pressure at 50 °C for several hours. Inside an argon-purged drybox, monomer and catalyst (400:1 molar ratio) were combined in a small tube with a single 24/40 ground glass opening and containing a magnetic stir bar. The tube was sealed with a Kontes high-vacuum valve adaptor and removed to a vacuum line, and the pressure was reduced in steps, ultimately reaching a dynamic vacuum of 10^{-2}−10^{-3} mmHg while increasing the temperature to 65 °C with magnetic agitation. Alternately, the reaction may be conducted in a pressure tube fitted with a vacuum valve via Teflon bushing, thereby eliminating the need to transfer the ADMET polymer to another vessel for hydrogenation. After 48 h, the vessel was sealed and returned to the drybox. In a glass pressure tube, the polymer/catalyst mixture was combined with silica gel-60 (100× the weight of catalyst) and sufficient toluene to aid dispersion (generally 10−15 mL for 500 mg of polymer). Hydrogen pressure was applied as quickly as possible, within 2−3 min, to deactivate the catalyst residue toward metathesis prior to dissolution of the polymer. The mixture was then heated to 90 °C with vigorous stirring while maintaining a constant pressure of 120 psig H_2 for 24 h. The mixture was filtered to remove the silica/catalyst residue composite, and the toluene evaporated to yield colorless viscous or water-white solid polymers.

ADMET/Hydrogenation of 11-Acetoxy-1,20-heneicosadiene (HP12). Elem. Anal. Calcd for $[C_{21}H_{40}O_2]$: C, 77.72; H, 12.42. Found: C, 77.63; H, 12.50. ^{1}H NMR δ (ppm): 4.83 (p, 1H); 2.02 (s, 3H); 1.50 (br, 4H); 1.23 (br, 32H). ^{13}C NMR δ: 170.9, 74.45, 34.15, 29.71, 29.58, 29.37, 25.33, 21.28. M_n (GPC vs PS) = 4.0×10^4 (PDI = 1.8).

ADMET/Hydrogenation of 12-Acetoxy-1,22-tricosadiene (HP13). Elem. Anal. Calcd for $[C_{23}H_{44}O_2]$: C, 78.35; H, 12.58. Found: C, 78.16; H, 12.63. ^{1}H NMR δ (ppm): 4.82 (p, 1H); 2.03 (s, 3H); 1.49 (br) + 1.25 (br) = 40H. ^{13}C NMR δ : 170.9, 74.42, 34.13, 29.65, 29.53, 29.29, 29.17, 25.31, 21.26. M_n (GPC vs PS) = 3.1×10^4 (PDI = 1.8).

ADMET/Hydrogenation of 13-Acetoxy-1,24-pentacosadiene (HP14). Elem. Anal. Calcd for $[C_{25}H_{48}O_2]$: C, 78.88; H, 12.71. Found: C, 78.83; H, 12.76. ^{1}H NMR δ (ppm): 4.83 (p, 1H); 2.01 (s, 3H); 1.47 (br) + 1.22 (br) = 44H. ^{13}C NMR δ: 170.9, 74.44, 34.11, 29.70, 29.58, 29.54, 25.31, 21.23. M_n (GPC vs PS) = 4.9×10^4 (PDI = 1.8).

ADMET/Hydrogenation of 15-Acetoxy-1,28-nonacosadiene (HP15). Elem. Anal. Calcd for $[C_{29}H_{56}O_2]$: C, 79.75; H, 12.92. Found: C, 79.61; H, 12.94. ^{1}H NMR δ (ppm): 4.83 (p, 1H); 2.01 (s, 3H); 1.47 (br, 4H); 1.22 (br, 48H). ^{13}C NMR δ: 170.8, 74.38, 34.10, 29.62, 29.56, 29.50, 29.09, 25.30, 21.29. M_n(GPC vs PS) = 6.6×10^4 (PDI = 1.8).

Acknowledgment. We thank the National Science Foundation, Division of Materials Research, for financial support of this work**.** We also thank Bob Hadba of the Department of Materials Science and Engineering (University of Florida) for graciously conducting GPC analysis.

References and Notes

(1) Zutty, N. L.; Faucher, J. A.; Bonotto, S. In *Encyclopedia of Polymer Science and Technology*; Mark, H. F., Ed.; John-Wiley and Sons: New York, 1967; pp 387−43.
(2) (a) Chowdhury, F.; Haigh, J. A.; Mandelkern, L.; Alamo, R. G. *Polym. Bull.* **1998**, *41*, 463−70. (b) Bistac, S.; Kunemann, P.; Schultz, J. *Polymer* **1998**, *39*, 4875−81. (c) Smith, G. D.; Liu, F.; Devereaux, R. W.; Boyd, R. H. *Macromolecules* **1992**, *25*, 703−8. (d) Buerger, D. E.; Boyd, R. H. *Macromolecules* **1991**, *22*, 2699.
(3) Ueda, A.; Nagai, S. In *Polymer Handbook*; Brandrup, J., Immergut, E. H., Grulke, E. A., Eds.; Wiley-Interscience: New York, 1999; Chapter II.
(4) (a) Gerum, W.; Höhne, G. W. H.; Wilke, W.; Arnold, M.; Wegner, T. *Macromol. Chem. Phys.* **1995**, *196*, 3797−3811. (b) Yakota, K.; Miwa, M.; Hirabayashi, T.; Inai, Y. *Macromolecules* **1992**, *25*, 5821−27. (c) Yakota, K.; Kouga, T.; Hirabayashi, T. *Polym. J* **1983**, *15*, 349−54. (d) Yakota, K.; Hirabayashi, T. *Macromolecules* **1981**, *14*, 1613−16.
(5) (a) McLain, S. J.; et al. *Proc. Am. Chem. Soc.: Div. Polym. Mater. Sci. Eng.* **1997**, *76*, 246. (b) Hillmyer, M. A.; Laredo, W. R.; Grubbs, R. H. *Macromolecules* **1995**, *28*, 6311−16.
(6) (a) Cho, I.; Moon, G. S. *J. Polym. Sci., Part A: Polym. Chem.* **1995**, *33*, 1823−28. (b) Cho, I.; Jo, S.-Y. *Macromolecules* **1999**, *32*, 521−23.
(7) (a) Wagener, K. B.; Valenti, D.; Watson, M. D. *Polym. Prepr.* (*Am. Chem. Soc., Div. Polym. Chem.*) **1998**, *39*, 719−720. (b) Valenti, D.; Wagener, K. B. *Macromolecules* **1998**, *31*, 2764−73. (c) Wagener, K. B.; Valenti, D.; Hahn, S. F. *Macromolecules* **1997**, *30*, 6688−90. (d) Smith, J. A.; Brzezinska, K. R.; Valenti, D.; Wagener, K. B. *Macromolecules* **2000**, *33*, 3781.
(8) Watson, M. D.; Wagener, K. B. *Macromolecules* **2000**, *33*, 3196.
(9) Schwab, P. F.; Marcia, B.; Ziller, J. W.; Grubbs, R. H. *Angew. Chem., Int. Ed. Engl.* **1995**, *34*, 2039.
(10) Flory, P. J. *Trans. Faraday Soc.* **1955**, *390* (51), 848.
(11) Sanchez, I. C.; Eby, R. K. *J. Res. Natl. Bur. Stand.* **1973**, *77A*, 353.
(12) Wunderlich, B. *J. Chem. Phys.* **1958**, *29*, 1395.
(13) Thermal properties of Elvax measured by differential scanning calorimetry (DSC). http://www.dupont.com/industrial-polymers/elvax/H-49653-1/H-49653-1.html. Accessed 01/2000.
(14) (a) Hoffman, J. D. *Polymer* **1983**, *23*, 4. (b) *Polymer* **1982**, *23*, 656.
(15) Marin, M. L.; Jimenez, A.; Lopez, J. *J. Therm. Anal.* **1996**, *47*, 247.

MA9920689